Resolution of the spectral technique in kinetic modeling

Chaincy Kuo, Bryan W. Reutter, and Ronald H. Huesman

Center for Functional Imaging, E.O. Lawrence Berkeley National Laboratory,
University of California.

ABSTRACT

Physiologic systems can be represented by compartmental models which describe the uptake of radio-labeled tracers from blood to tissue and their subsequent washout. Arterial and venous time-activity curves from isolated heart experiments are analyzed using spectral analysis, in which the impulse response function is represented by a sum of decaying exponentials. Resolution and uniqueness tests are conducted by synthesizing isolated heart data with predefined compartmental models, adding noise, and applying the spectral analysis technique. Venous time-activity curves are generated by convolving a typical arterial input function with the predefined spectrum. The coefficients of a set of decaying exponential basis functions are determined using a non-negative least squares algorithm, and results are compared with the predefined spectrum. The uniqueness of spectral method solutions is investigated by computing model covariance matrices, using error propagation and prior knowledge of noise distributions. Coupling between model parameters is illustrated with correlation matrices.

Keywords: Spectral analysis–Kinetic modeling

1. INTRODUCTION

Time-activity curves are modeled by convolving the blood input function with an impulse response function, which characterizes the transport of tracer of interest in living tissue. Compartmental analysis is a useful method of modeling physiology, but requires *a priori* information on the appropriate kinetic model describing the physiologic processes. Without the proper *a priori* assumptions, misguided conclusions may be drawn regarding physiologic structure. Data quality also limits the precision to which the model structure may be retrieved.

As an alternative, we continue to investigate the utility of spectral analysis techniques used to determine the appropriate delineation of physiologic processes in tissues of interest. As outlined by Cunningham and Jones [1], the general approach of spectral analysis is to model the impulse response function as a sum of a large number of decaying exponential terms, the coefficients of which are non-negative. Modeling assumptions are thus minimized by using this large set of model parameters.

The accuracy of the retrieved spectral components will be addressed. The sensitivity of the spectral method can be evaluated by investigating the nature of results from the spectral method. Turkheimer et al.[2] have used bootstrapping techniques to assess uncertainty in washout parameters from PET studies using spectral analysis. Bertoldo et al.[3] have inspected the inverse of the Fisher information matrix to evaluate precision of uptake parameters from spectral analysis of PET data. In this study, the precision of spectral method uptake and washout parameters will be investigated by computing model covariance matrices, using error propagation and prior knowledge of noise distributions. Coupling between model parameters can be illustrated with correlation matrices. Synthetic time-activity curves will be forward-modeled by convolving the synthetic impulse response function with a blood input functional form. Synthetic curves simulate data from experiments utilizing the isolated rabbit heart model [4]. In these heart experiments, data are acquired by sampling the venous blood after introduction, via the aorta, of constant proportions of a tracer of interest and a reference tracer (albumin), which does not leave the vasculature.

Further author information: (Send correspondence to C.K.)
E.O. Lawrence Berkeley National Laboratory, 1 Cyclotron Road #55-121, Berkeley, CA, 94720; http://cfi.lbl.gov
C.K.: E-mail CKuo@lbl.gov;phone 1 510 486 6762
B.W.R.: E-mail BWReutter@lbl.gov; phone 1 510 486 4265
R.H.H.: E-mail RHHuesman@lbl.gov; phone 1 510 486 4062

2. METHOD

2.1. Time Activity Curves

The time-activity of perfused tracer in tissue is modeled by convolving in the time domain a blood input function $I(t)$ with an impulse response function $R(t)$. That is,

$$\Omega(t) = \int_0^t I(t-t')R(t')dt'. \tag{1}$$

The radio-labeled tracer concentration in venous blood flowing from isolated heart experiments is collected over finite time intervals. The acquisition can be expressed as

$$D_i = \frac{1}{t_i - t_{i-1}} \int_{t_{i-1}}^{t_i} \Omega(t)dt \tag{2}$$

where the t_i's are the endpoints of acquisition time intervals, and $i = 1, 2, 3, ...N$ and N is defined by $t_{tot} = t_N - t_0$ where t_{tot} is the total acquisition time, and t_0 is the acquisition start time.

2.2. Synthetic Time Activity Curves

Time activity curves are simulated in order to assess the spectral methodology. Synthetic time activity curves are computed by convolving functional forms of $I(t)$ and $R(t)$ in the time domain.

In order to synthesize the blood input function, we use the functional form

$$I(t) = \alpha t^n e^{\beta t} \tag{3}$$

for the input blood curve. The synthetic impulse response function $R^s(t)$ then was modeled in two forms:

- as a sum of decaying exponentials

$$R^s(t) = \sum_{k=1}^{n_s} x_k^s \frac{e^{-t/\tau_k^s}}{\tau_k^s} \tag{4}$$

  where n_s is a small number of decaying exponentials, and

- as an integration over continuous spectral function:

$$R^s(t) = \left(\frac{1}{\tau_2} - \frac{1}{\tau_1}\right)^{-1} \int_{\frac{1}{\tau_1}}^{\frac{1}{\tau_2}} \frac{e^{-t/\tau}}{\tau} d\left(\frac{1}{\tau}\right). \tag{5}$$

  The x_k in the range of integration are set to 1, and the integration is performed over $1/\tau$ as we wish to generate uniformity in rate λ, where $\lambda = 1/\tau$. On the other hand, in τ-space, the x_k's should fall off as a function of $1/\tau^2$.

The synthetic time-activity curves, $\Omega^s(t)$, are convolved numerically in the time domain, and we synthesize the data D_i^s by defining an acquisition time schedule for concentration of the tracer of interest (Equation (2)) in accordance with typical isolated heart studies. Normally distributed random noise is then added to each time point D_i^s. By specifying variances for each measurement D_i^s, the errors can be propagated so that it will be possible to define uncertainties for model parameters x_k and τ_k.

2.3. Model estimation

Adopting the spectral approach, the mean value of the data can be predicted by

$$\mathbf{b} = \mathbf{A}\mathbf{x} \tag{6}$$

where $\mathbf{b}$ is a vector of time activity, $\mathbf{x}$ is the vector of tracer amounts defined in Equation (7), and $\mathbf{A}$ is the data kernel matrix.

In the forward problem, data from isolated heart reference tracer time-activity are measured for $I(t)$, and the impulse response function is expressed as a sum of decaying exponentials

$$R(t) = \sum_{k=1}^{K} x_k \frac{e^{-t/\tau_k}}{\tau_k}, \tag{7}$$

where the coefficients x_k and τ_k represent, respectively, amount of tracer uptake and time constant of tracer washout by channel k. The x_k's are required to be positive values or zero. The lower and upper bound for the range of time constant τ_k is chosen in accord with physiologically reasonable values and experimental design. The τ interval is segmented evenly on a logarithmic scale, where the choice $\tau_k = 1.1^k$ (seconds) has been made here, and $K = 98$. Thus, $\tau_k = [1.10s, 1.21s, \ldots, 11388.94s]$. A single exponential function indexed by k shall be referred to as $R_k(t)$.

The elements of $\mathbf{A}$ are then

$$A_{ik} = \int_{t_{i-1}}^{t_i} \int_0^t I(t') \frac{e^{-(t-t')/\tau_k}}{\tau_k} dt' dt \tag{8}$$

where $i = 1, 2, \ldots, N$ and $k = 1, \ldots, K$. $I(t')$ is modeled to be piecewise constant over each time interval $t' = [t'_{i-1}, t'_i]$. One additional column of $\mathbf{A}$ contains the piecewise constant values of $I(t)$, and another column is populated with 1's, for a constant DC component, bringing the total number of columns in $\mathbf{A}$ to 100.

Then, given a synthetic time series of D_i^s's, the minimum of the criterion

$$\begin{aligned} E &= (\mathbf{D}^s - \mathbf{b})^T \mathbf{W}^{-1} (\mathbf{D}^s - \mathbf{b}) \\ &= (\mathbf{D}^s - \mathbf{A}\mathbf{x})^T \mathbf{W}^{-1} (\mathbf{D}^s - \mathbf{A}\mathbf{x}) \end{aligned} \tag{9}$$

is sought, subject to the constraint that $\mathbf{x} \geq 0$. $\mathbf{W}$ is a weighting matrix consisting of data covariance estimates. $\mathbf{W}$ is diagonal as the activity measurements at each time point are independent of each other. We use a non-negative weighted least-squares algorithm [5] to estimate the spectral values $\mathbf{x}$. The non-negativity constraint is used to help stabilize the solution. Estimates for which $x_k > 0$ are often interpreted to correspond with identification of washout rates τ_k's.

2.4. Covariance and Correlation

The non-negative least squares algorithm which we employ, NNLS by Lawson and Hanson [5], solves the problem $\mathbf{A}_R \mathbf{x}_R = \mathbf{b}$ for the solution vector $\mathbf{x}_R$ in which all elements of $\mathbf{x}_R > 0$. The matrix $\mathbf{A}_R$ is reduced from $\mathbf{A}$ such that it consists of the columns of $\mathbf{A}$ corresponding to positive values in $\mathbf{x}$. The covariance of model parameters $\mathbf{x}_R$ can then be calculated from

$$\begin{aligned} [\mathbf{cov}\, \mathbf{x_R}] &= (\mathbf{A}_R^T \mathbf{W}^{-1} \mathbf{A}_R)^{-1} \mathbf{A}_R^T \mathbf{W}^{-1} [\mathbf{cov}\, \mathbf{D}^s] \mathbf{W}^{-1} \mathbf{A}_R (\mathbf{A}_R^T \mathbf{W}^{-1} \mathbf{A}_R)^{-1} \\ &= (\mathbf{A}_R^T \mathbf{W}^{-1} \mathbf{A}_R)^{-1}, \end{aligned} \tag{10}$$

where $[\mathbf{cov}\, \mathbf{D}^s]$ is the covariance matrix of data vector $\mathbf{D}^s$ and is equal to the diagonal weighting matrix $\mathbf{W}$.

Typically, the spectral technique returns estimates for $x_k > 0$ which either have non-zero neighbors, or are isolated, with neighboring zero values ($x_{k-1} = x_{k+1} = 0$). How are the τ_k corresponding to non-zero x_k's considered to be either coupled or isolated? Neighboring non-zero x_k's could be considered to be coupled. But without uncertainty measurements for time constants τ, the resolution of the spectral technique when analyzing tracer kinetics would be indicated by the segmentation of τ, or inversely, of washout rate constant $\lambda = 1/\tau$, in the basis set. As the segmentation width of the basis set is specified by the investigators, the space spanned by the basis functions may be either redundant or incomplete. We calculate the correlation coefficient $\varsigma_{k,k'}$ between model parameters x_k and $x_{k'}$ as this can offer insight into coupling between basis functions $R_k(t)$ and $R_{k'}(t)$.

We assume that the $R_k(t)$'s corresponding to x_k's correlated in series are coupled and compute a central value τ_c by taking an average of τ_k's weighted by their corresponding x_k's. That is, given a criterion value κ defining correlation, a combined τ_c for which $|\varsigma_{k,k+1}| > \kappa$, $|\varsigma_{k,k+2}| > \kappa$, to $|\varsigma_{k,k+J}| > \kappa$, is specified by

$$\tau_c = \frac{\sum_{j=0}^{J} x_{k+j}\,\tau_{k+j}}{\sum_{j=0}^{J} x_{k+j}}. \tag{11}$$

The variance of the combined τ_c value can then be computed with

$$\sigma^2_{\tau_c} = \sum_{m=0}^{J}\sum_{n=0}^{J}\left(\frac{\partial \tau_c}{\partial x_{k+m}}\right)\sigma^2_{x_{k+m,k+n}}\left(\frac{\partial \tau_c}{\partial x_{k+n}}\right). \tag{12}$$

The combined amplitude x_c and $\sigma^2_{x_c}$ corresponding to τ_c are simply

$$x_c = \sum_{j=0}^{J} x_{k+j}\,, \tag{13}$$

and

$$\sigma^2_{x_c} = \sum_{i=0}^{J}\sum_{j=0}^{J}\sigma^2_{x_{k+i\,k+j}}. \tag{14}$$

3. SIMULATION RESULTS AND DISCUSSION

In the simulations which follow, a realization for the input blood function is composed by fitting the coefficients α, β, and n as defined in Equation (3) to data from a particular isolated heart experiment [4]. The values $\alpha = 0.001832$, $\beta = 0.521914$, and $n = 7.432533$ were estimated by using a simplex fitting package from MATLAB (The Mathworks, Sherborn, MA). These values are used to model the input blood curve in all subsequent tests.

Impulse response functions are specified for isolated spectra, and for a spectral continuous function. The impulse response function for each will be detailed in the following sections describing the experiment. The data acquisition schedule of a typical heart study is approximately $t_i = 4$ seconds for the first 180 seconds of acquisition, then $t_i = 7$ seconds up to 600 seconds of acquisition, and then $t_i = 10$ seconds until 1800 seconds of acquisition.

3.1. Individual Spectra

We investigate the sensitivity of our method with impulse response functions expressed as individual and separate components, according to Equation (7).

3.1.1. Single peak

In this first experiment, the impulse response function is defined by Equation 7 such that $n_s = 1$, $x_1^s = 1$, and $\tau_1^s = 100\,s$. Gaussian distributed random noise was added to the output response function at the 10% level. Keeping in mind the dynamic range of realistic measurement error, the uncertainties in the measurement were the chosen to be 10% of D_i^s, and allowed to asymptotically approach a predefined minimum value of uncertainty as D_i^s decreased to very small values. These uncertainties were used as weights in the non-negative least squares routine.

Figure 2a displays the results of the NNLS for a basis set in which the range of $\tau_k = [1.1, 1.1^2, \ldots, 1.1^{98}]$ seconds. There are two adjacent components in the neighborhood of $\tau = 100\,s$. Using Equations (11)–(14), we find for this realization of the synthetic data, that

$$\begin{aligned} x_c &= 1.0233 \pm 0.0106 \\ \tau_c &= 98.9308 \pm 0.1103 \end{aligned}$$

The standard deviations computed by Equations (11)–(14) for this one realization of data are in agreement with the statistics of x_c and τ_c results from 1000 Monte Carlo generations of synthetic data. Figure 1 shows histograms of x_c's, σ_{x_c}'s, τ_c's, and σ_{τ_c}'s computed from each of the 1000 NNLS solutions.

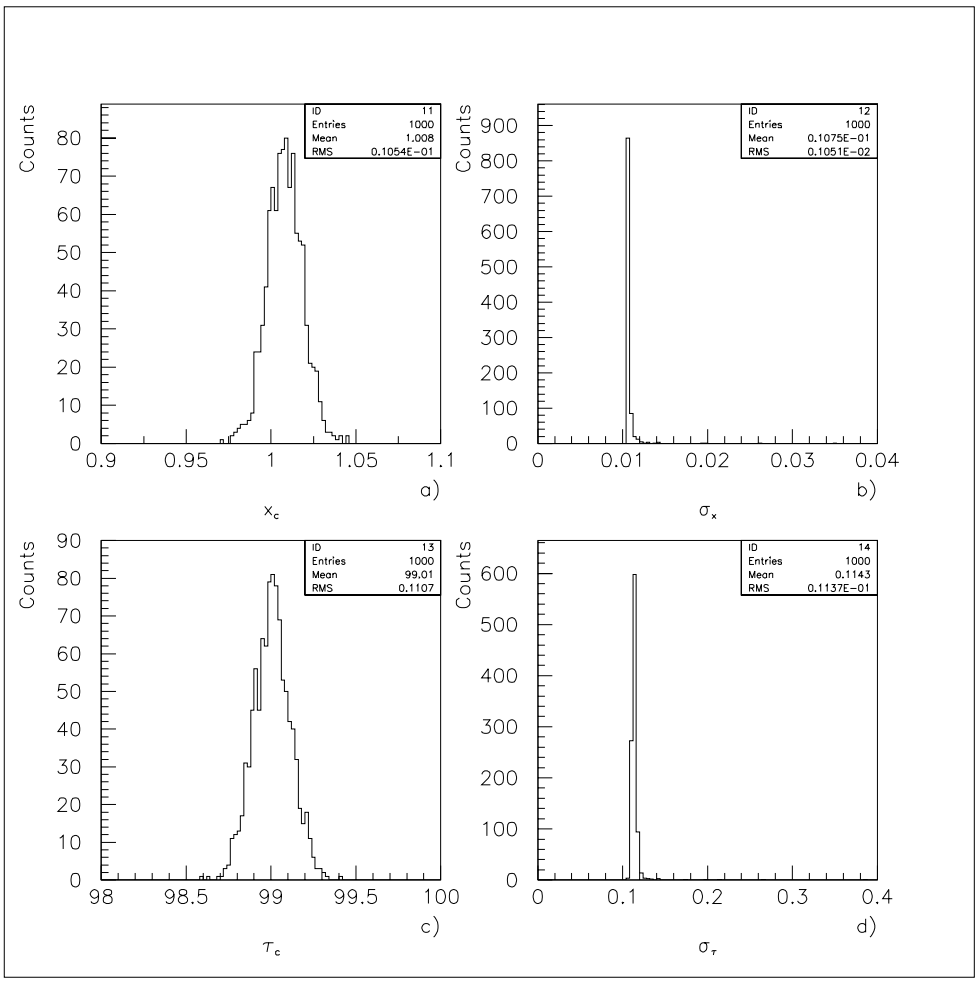

Figure 1. Histograms of combined a) x_c's, b) σ_{x_c}'s, c) τ_c's, and d) σ_{τ_c} determined from 1000 Monte Carlo generations of synthetic data. The mean and standard deviations of each histogram are a) $\langle x_c \rangle = 1.008 \pm 1.054 \times 10^{-2}$, b) $\langle \sigma_{x_c} \rangle = 1.075 \times 10^{-2} \pm 1.051 \times 10^{-3}$, c) $\langle \tau_c \rangle = 99.01 \pm 1.107 \times 10^{-1}$ d) $\langle \sigma_{\tau_c} \rangle = 1.143 \times 10^{-1} \pm 1.137 \times 10^{-2}$.

3.1.2. Basis set shift

In order to determine the sensitivity of Equation (11) to the basis set, we test Equation (11) by using 10 different basis sets. To do so, we shift the time constant τ_k range on the logarithmic scale, while preserving the τ interval as previously defined, so that τ_k now becomes

$$\tau_k = (1 + n_\xi \xi) 1.1^k, \tag{15}$$

where ξ is a shift increment, and n_ξ is a shifting factor. Then a given amount of basis set shift is $n_\xi \xi$. We define the shift increment to be $\xi = 0.01$, so that for $n_\xi = 0$ and $n_\xi = 10$, the basis sets would consist of functions with the same time constants, differing only at the first and last τ_k.

For the same realization of data as in Section 3.1.1, Figure 2 shows the results of the weighted NNLS in finding x_k values for the τ_k's in each basis set defined by its n_ξ. Note that in the neighborhood of $\tau = 100\,s$, when the τ_k's straddle $\tau = 100\,s$ as in Figure 2h, the non-zero x_k's become close to equal in value, as one would expect. As the use of all basis sets returns two adjacent non-zero x_k values from the weighted NNLS, we can compute an x_c and τ_c and their corresponding standard deviations, and they are displayed in Figures 3a and 3b for each basis set. x_c, τ_c, and χ^2 vary smoothly as the basis set is increasingly shifted (i.e., as n_ξ increases), except for the cusp at $n_\xi = 3$. For this basis set, $n_\xi = 3$, x_c and χ^2 are minimized while τ_c reaches a peak. In this basis set, there is a $\tau_k \approx 100\,s$ which is closer to the value of τ_1^s defined in this test than in the other basis sets. At $n_\xi = 4$ however, the uncertainties σ_{x_k} and σ_{τ_k} experience a sharp increase. In Figures 2c–e, we see that the larger x_k in the pairs of channels switches

from being the left of the pair to being the right. Although there appears to be only a single channel in the solution in Figure 2d, $x_k \sim 10^{-3}$ to the right of the large channel. For $n_\xi < 4$, the solution x_k's fall on $\tau_k \sim 100\,s$ and $\tau_{k+1} \sim 110\,s$. As the basis τ_k's are increasingly shifted, at $n_\xi = 4$, the solution falls back on $\tau_k \sim 90\,s$ and $\tau_k \sim 100\,s$. $\sigma^2_{x_k}$'s are larger for lower valued τ_k channels as they are more closely spaced on a linear scale. As the basis set shifts, the solution also shifts to include a lower value τ_k, which gives a $\sigma^2_{x_k}$ estimation, and in turn, from Equation (12), also results in a higher $\sigma^2_{\tau_k}$. Then, as the basis set has "reset" and continues to increasingly shift, the inclusion of higher τ_k, and therefore lower variances on x_k, is gradual.

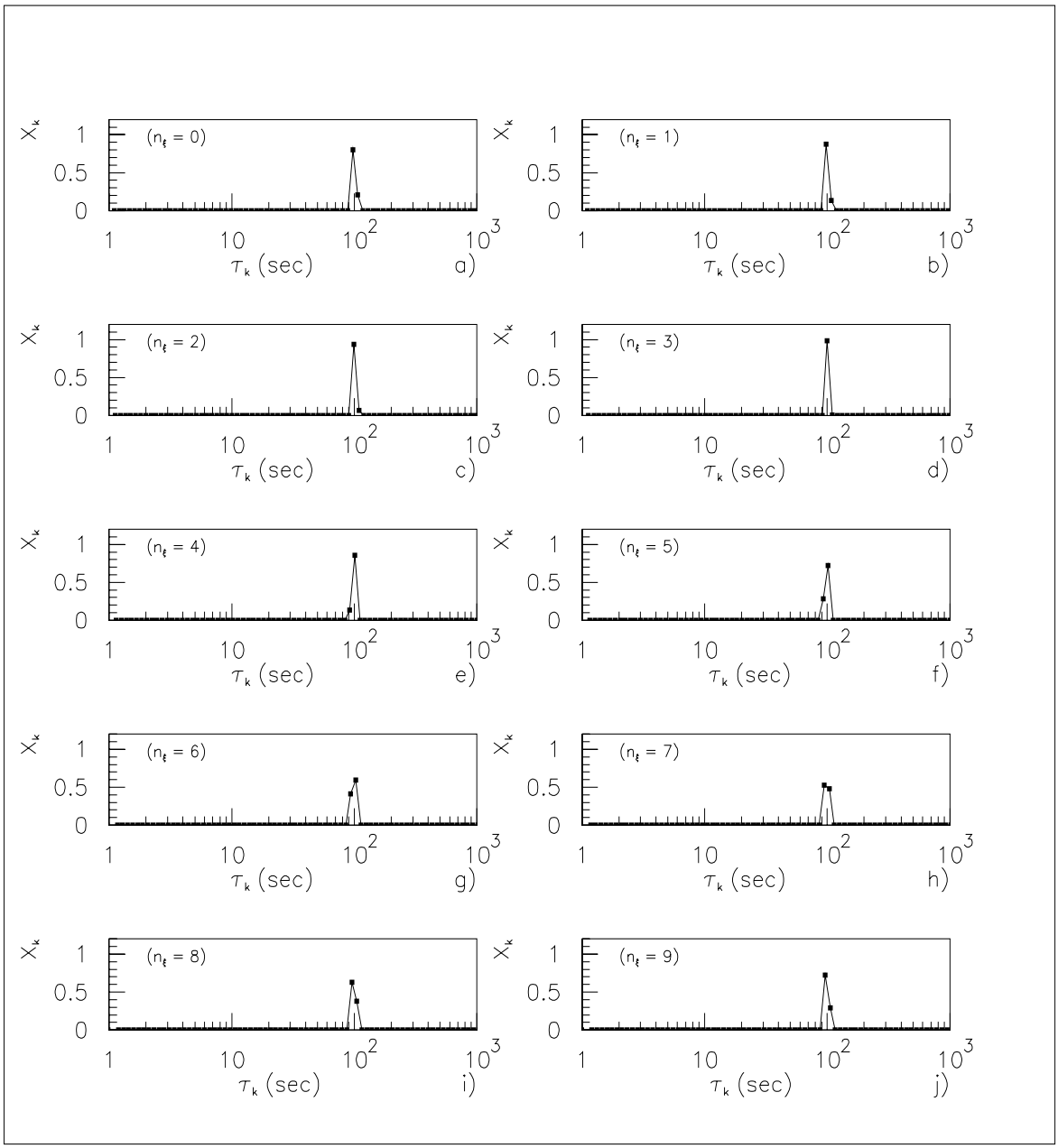

Figure 2. a)–j) 10 different basis sets are used to estimate x_k from NNLS. τ_k for each set is defined by Equation 15. $x^s_k = 1, \tau^s_k = 100\,s$ are used in simulating data, with 10% Gaussian random noise. Weights are described in the text. The square marker indicates the values of the solution vector $\mathbf{x}$. Note that neighboring zero values of x_k appear to be a bold solid line along the abscissa.

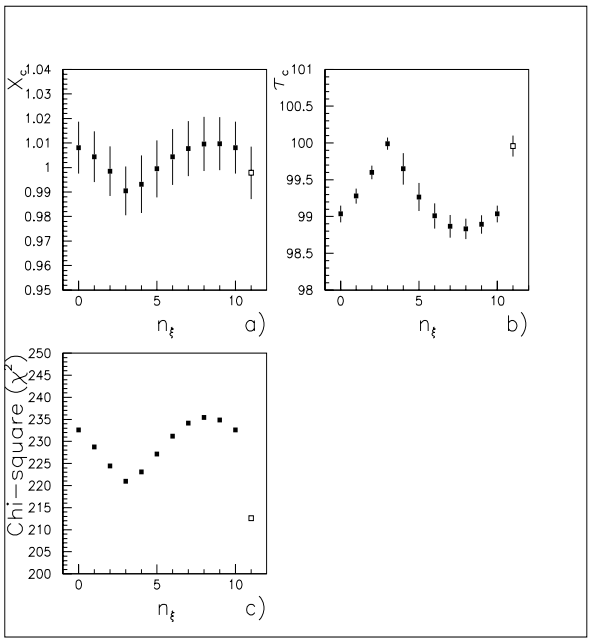

Figure 3. a) x_c b) τ_c and c) χ^2 are plotted for $0 \leq n_\xi \leq 10$ with closed square markers. The results of RFIT for this realization of data is plotted at $n_\xi = 11$ with the open square marker.

At $n_\xi = 11$ in Figures 3a–c, the results of the shifting basis set tests are compared to computations from RFIT [6], an application which estimates parameters for a predefined compartmental model from a closed form solution of $D(t)$ [7]. RFIT also reports uncertainties for the model parameter estimates. The spectral technique defines a grid upon which the solutions must lie, whereas RFIT has freedom to estimate parameters in continuous space. Given that the forward models differ between RFIT and the spectral technique, the uncertainty values computed by both methods are in good correspondence.

3.1.3. Multiple components

As tissue is typically heterogeneous rather than homogeneous, we now investigate Equation (7) such that $n_s = 2$, $x_1^s = x_2^s = 1$, $\tau_1^s = 50\,s$, and $\tau_2^s = 100\,s$. 20% Gaussian noise was added to the synthetic, and the weights were defined using the same consideration as described in Section 3.1.1, except for 20% of $D^s(t)$.

From one realization of synthetic data, the weighted NNLS routines returns two sets of coupled channels,

channel	x_k	$\tau_k\ s$
1	$1.3940e-01$	41.1448
2	$7.1842e-01$	45.2593
3	$9.3502e-01$	97.0173
4	$1.5272e-01$	106.7190,

as seen in Figure 4a. The coupling can be defined either by the observation that the channels are adjacent to each other in the spectrum, or by inspecting the correlation between the non-zero x_k's:

	ς_{x_1}	ς_{x_2}	ς_{x_3}	ς_{x_4}
ς_{x_1}	$1.0000e+00$			
ς_{x_2}	$\mathbf{-9.9536e-01}$	$1.0000e+00$		
ς_{x_3}	$5.1504e-01$	$-5.5346e-01$	$1.0000e+00$	
ς_{x_4}	$-4.2482e-01$	$4.5795e-01$	$\mathbf{-9.3976e-01}$	$1.0000e+00.$

If the correlation criterion is determined so that $|\varsigma_{k\,k'}| > \kappa$ defines coupling, and we set $\kappa = 0.9$, then we can see by the boldface values in the correlation matrix that channels 1 and 2 and channels 3 and 4 are coupled. Then for

each coupled pair, we find the values listed in (Table 1) and compare them with statistics of 1000 Monte Carlo (MC) tests, and find good agreement.

Table 1. Comparison of results from one realization of a synthetic, $n_s = 2$, $x_1^s = x_2^s = 1$, $\tau_1^s = 50\,s$, and $\tau_2^s = 100\,s$, to statistics of 1000 Monte Carlo runs.

	x_c	σ_{x_c}	$\tau_c\ s$	σ_{τ_c}	J
	8.578e-01	± 7.626e-02	44.591	± 3.7867	2
	1.088e+00	± 3.842e-02	98.379	± 0.2895	2
MC	8.636e-01	± 1.360e-01	48.19	± 4.313	N/A
	1.055e+00	± 4.420e-02	98.58	± 0.3004	N/A

3.2. Continuous Spectral Model

Spectral analysis of tracer kinetic data has in general retrieved a small (< 5) number of exponential components [1,4,8]. The robustness of the spectral technique is investigated with impulse response functions which are defined as an integral over a continuous range of exponential functions of equal amplitude. The spectrum of such an impulse response function is a continuous function in exponential decay constant space.

We specify the impulse response function as an integration of a continuous function, according to Equation (5), with $\tau_1 = 50\,s$ and $\tau_2 = 100\,s$. 20% noise is added to the synthetic, and the weights are designated as previously described. The weighted NNLS returns the solution shown in Figure 4b. Rather than returning a large number of neighboring peaks continuously distributed over the continuous range, the inversion returned a small number (~ 5) of discrete spectral peaks distributed over the continuous range. There are actually 6 non-zero values in $\mathbf{x}$. The first $x_1 \sim 10^{-8}$ in the DC channel. Inspecting the correlation matrix,

	ς_{x_1}	ς_{x_2}	ς_{x_3}	ς_{x_4}	ς_{x_5}	ς_{x_6}
ς_{x_1}	$1.0000e+00$					
ς_{x_2}	$-3.0520e-01$	$1.0000e+00$				
ς_{x_3}	$3.3408e-01$	$\mathbf{-9.9373e-01}$	$1.0000e+00$			
ς_{x_4}	$-3.6639e-01$	$\mathbf{9.7364e-01}$	$\mathbf{-9.9280e-01}$	$1.0000e+00$		
ς_{x_5}	$4.8229e-01$	$-8.4530e-01$	$8.9115e-01$	$\mathbf{-9.3337e-01}$	$1.0000e+00$	
ς_{x_6}	$-5.2712e-01$	$7.9744e-01$	$-8.4627e-01$	$8.9356e-01$	$\mathbf{-9.9197e-01}$	$1.0000e+00$

we see that, given the criterion for correlation $\kappa = 0.9$, each channel is not only correlated with its neighbor, but each is also correlated with the next channel in the sequence.

The separation of channel clusters is distinct in the example given in Section 3.1.3, while the correlation between channel clusters is notable in Section 3.2 and gives indication towards a continuous range of τ_k's. For narrower window limits, $\tau_1 = 70\,s$ and $\tau_2 = 100\,s$ for example, distinguishing between a continuous range of τ_k's and distinctly separate τ_k's becomes impossible, as the behavior of the correlation matrices in each case is similar. That is, there is high correlation between solution x_k's. The correlation matrices are not shown in the interest of conserving space. On the other hand, the correlation matrices may be useful in determining τ range segmentation–that is, τ_k bin width. In future investigations, the correlation matrix behavior will be evaluated as the bin width is modified, in hopes of reducing redundancy in the span of the basis set.

4. CONCLUSIONS

Spectral decomposition in general refers to systems for which the bases which span the system space are orthogonal functions. In the case of the basis set comprised of 100 decaying exponentials, which is utilized for this kinetic spectral analysis, there is a redundancy in the expression of the feasible solution space.

Analysis of real biological data may not allow the refined precision of spectral intervals defined in our exponential basis set, due to the presence of noise, and the data acquisition procedures. Although there are acquisition gaps in

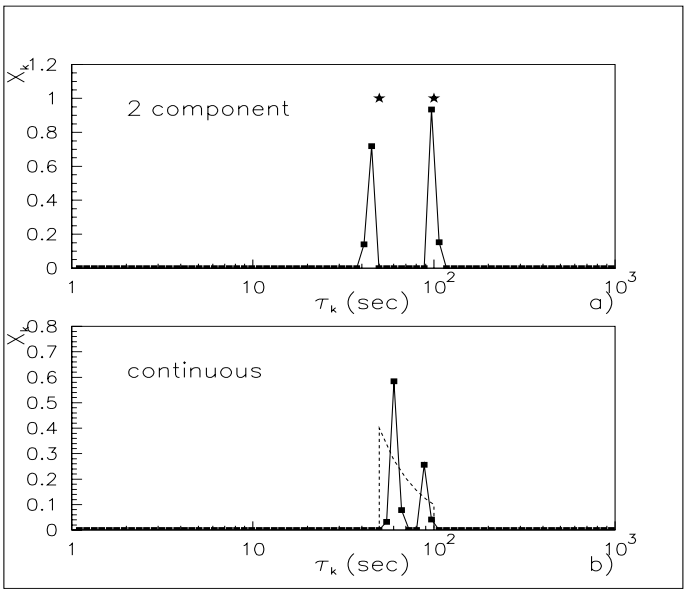

Figure 4. Estimates for x_k from NNLS. The basis set used is one for which $n_\xi = 0$. a) plotted with stars, $x_1^s = 1, \tau_1^s = 50\,s, x_2^s = 1, \tau_2^s = 100\,s$ are defined for the data simulation, with 20% Gaussian random noise. b) The impulse response is defined according to Equation 5, using limits $\tau_1 = 50\,s$ and $\tau_2 = 100\,s$, and plotted with a dashed line. The square marker indicates the values of the solution vector $\mathbf{x}$.

the late times in actual heart experiments, where the time activity of tracer concentration has stabilized and the gradient is very small, we do not simulate these gaps, and take data continuously. As a result, the synthetic data set includes more time points than a typical heart study.

Model covariance matrices which include the variance of the data have been computed to assess the precision of model parameter estimates x_k. By doing so, we have also measured central time constants τ_c and their variances. It has been demonstrated that there is good correspondence between our measurements of σ_τ^2 and σ_x^2, and uncertainties estimated from separate methods [6] used to determine kinetic model parameters. Model covariance matrices were also used to investigate the correlations between model parameters set up by the modeling theory in the synthetic tests. Correlation matrices may be useful in determining the basis set bin width which could reduce redundancy in basis functions.

ACKNOWLEDGMENTS

This work was supported by the National Heart, Lung, and Blood Institute of the US Department of Health and Human Services under grant P01-HL25840; and by the Director, Office of Science, Office of Biological and Environmental Research, Medical Sciences Division of the US Department of Energy under contract DE-AC03-76SF00098.

DISCLAIMER

REFERENCES

1. V. J. Cunningham and T. Jones, "Spectral analysis of dynamic PET studies," *J. Cereb. Blood Flow Metab.*, **13**, pp. 15–23, 1993.
2. F. Turkheimer, L. Sokoloff, A. Bertoldo, G. Lucignani, M. Reivich, J. L. Jaggi, and K. Schmidt.,"Estimation of component and parameter distributions in spectral analysis," *J. Cereb. Blood Flow Metab.*, **18**, pp. 1211–1222, 1998.
3. A. Bertoldo, P.V. Vicini, G. Sambuceti, A.A. Lammertsma, O. Parodi, and C. Cobelli, "Evaluation of compartmental and spectral analysis models of [^{18}F]FDG kinetics for heart and brain studies with PET," *IEEE Trans. Biomed. Eng.*, **45**, pp. 1429-1448, 1998.
4. R. C. Marshall, P. Powers-Risius, B. W. Reutter, S. E. Taylor, H. F. VanBrocklin, R. H. Huesman, and T. F. Budinger,"Kinetic analysis of ^{125}I-iodorotenone as a deposited myocardial flow tracer: comparison to ^{99m}Tc-sestamibi," *J. Nucl. Med.*,**42**, 2001.
5. C. L. Lawson and R. J. Hanson, *Solving least squares problems*, Prentice-Hall, Englewood Cliffs, 1974.
6. R. H. Huesman, B. L. Knittel, B. M. Mazoyer, P. G. Coxson, E. M. Salmeron, G. J. Klein, B. W. Reutter, and T. F. Budinger ,"Notes on RFIT: a program for fitting compartmental models to regions-of-interest dynamic emission tomography data," Report LBL–37621, E.O. Lawrence Berkeley National Laboratory, 1993.
7. P. G. Coxson, E. M. Salmeron, R. H. Huesman, and B. M. Mazoyer, "Simulation of compartmental models for kinetic data from a positron emission tomograph," *Comput. Methods Programs Biomed.*, **37**, pp. 205–214, 1992.
8. F. Turkheimer, R. M. Moresco, G. Lucignani, L. Sokoloff, F. Fazio, and K. Schmidt,"The use of spectral analysis to determine regional cerebral glucose utilization with positron emission tomography and [^{18}F]Fluorodeoxyglucose: theory, implementation, and optimization procedures," *J. Cereb. Blood Flow Metab.*, **14**, pp. 406–422, 1994.